

# *N*-Glycosylamines of 4,6-*O*-ethylidene- $\alpha$ -D-glucopyranose: synthesis, characterisation and structure of CO<sub>2</sub>H, Cl and F *ortho*-substituted phenyl derivatives and metal ion complexes of the CO<sub>2</sub>H derivative †

Ajay K. Sah,<sup>a</sup> Chebrolu P. Rao,<sup>\*a</sup> Pauli K. Saarenketo,<sup>b</sup> Elina K. Wegelius,<sup>b</sup> Kari Rissanen<sup>b</sup> and Erkki Kolehmainen<sup>b</sup>

<sup>a</sup> *Bioinorganic Laboratory, Department of Chemistry, Indian Institute of Technology, Bombay, Powai, Mumbai-400 076, India. Fax: (+91-22) 572 3480; E-mail: cprao@ether.chem.iitb.ernet.in*

<sup>b</sup> *Department of Chemistry, University of Jyväskylä, Jyväskylä, Fin 40351, Finland*

Received 19th June 2000, Accepted 30th August 2000

First published as an Advance Article on the web 3rd October 2000

A saccharide based ligand suitable for metal binding (HL<sub>COOH</sub>) has been synthesized using 4,6-*O*-ethylidene- $\alpha$ -D-glucopyranose (4,6-*O*-EGP) and anthranilic acid. A few analogous glycosylamines with chloro and fluoro *ortho* substitutions have also been synthesized and characterised. Complexes of HL<sub>COOH</sub> with Na<sup>+</sup>, K<sup>+</sup>, Mg<sup>2+</sup>, Ca<sup>2+</sup>, Ba<sup>2+</sup>, Cd<sup>2+</sup> and Hg<sup>2+</sup> have been isolated and characterised fully. The crystal structures of 4,6-*O*-EGP, the chloro analogue of HL<sub>COOH</sub> and the K<sup>+</sup> complex of L<sub>COOH</sub> are established. The anomeric nature, orientation of the binding core and the co-ordination aspects of K<sup>+</sup> have been derived from these structures.

## Introduction

Knowledge regarding the chemistry of interaction of metal ions with saccharides is of potential importance to the field of inorganic chemistry in general and bioinorganic chemistry in particular, due to the fact that both saccharides and metal ions coexist in biological systems.<sup>1,2</sup> Only during the past decade or so, the literature is concerned mainly with the characterisation of the isolated products of interaction of transition metal ions with simple saccharides.<sup>3</sup> However, the understanding of these interactions was limited due to the lack of crystal structures of sufficient metal ion–saccharide complexes. This problem can partly be circumvented *via* modifying the saccharides either by selectively blocking some OH groups or by modifying these through glycosylation at position C1 or by a combination of both.<sup>4–7</sup> Some recent literature reports include crystal structures of glucose based platinum(IV) complexes by Steinborn's group<sup>8</sup> and metal ion complexes of 1,2- and 5,6-blocked glucopyranose by the groups of Floriani, Duthaler and Togni.<sup>6,9,10</sup> Jäger, Klemm and co-workers have recently communicated bi- and tri-nuclear copper complexes of a glucose based  $\beta$ -oxoamine ligand.<sup>11</sup> On the other hand, Yano's group has reported crystal structures of a number of transition metal ion complexes of C1–N glycosides derived from the reactions of glucose and different amines.<sup>7,12</sup> Leary's group has reported only the structure of an aminoglycoside ligand derived from diethylenetriamine and demonstrated the interaction of this with Zn<sup>2+</sup> based on mass spectral data.<sup>13a</sup> All the metal ion complexes of the glycosylamines reported are ionic in nature. However, there have been hardly any literature reports regarding metal ion complexes of glycosylamines derived from aromatic amines possessing *ortho* functionalities, which are expected to enhance the metal ion binding characteristics of the corresponding saccharides. Therefore, in this paper we report the synthesis and characterisation of a series of 4,6-*O*-ethylidene- $\alpha$ -D-glucopyranose

(4,6-*O*-EGP) based aromatic glycosylamines possessing *ortho* substitutions. Further this paper also deals with the synthesis, and analytical and spectral characterisations, of complexes of *N*-(*o*-carboxyphenyl)-4,6-*O*-ethylidene- $\beta$ -D-glucopyranosylamine with Na<sup>+</sup>, K<sup>+</sup>, Mg<sup>2+</sup>, Ca<sup>2+</sup>, Ba<sup>2+</sup>, Cd<sup>2+</sup> and Hg<sup>2+</sup> ions. The potassium complex has been characterized by single crystal X-ray diffraction.

## Experimental

Glucose was procured from Aldrich Chem. Co. (USA), amines from Lancaster Synthesis Ltd (UK) and paraldehyde from BDH (UK). All the solvents were purified and dried immediately before use. Elemental analysis was carried out on a Carlo-Erba elemental analyser and FTIR spectra were recorded on a Nicolet Impact 400 machine. TGA/DTA studies were carried out on a Perkin-Elmer TGA7/DTA7 System. <sup>1</sup>H NMR spectra were recorded on a Bruker Avance DRX 500 spectrometer in (CD<sub>3</sub>)<sub>2</sub>SO.

## Synthesis of ligands

**4,6-*O*-ethylidene- $\alpha$ -D-glucopyranose (4,6-*O*-EGP).** This was prepared by a literature procedure using 200 mmol D-glucose.<sup>14</sup> The crystalline product was isolated in two crops. This compound was also synthesized on a 2000 mmol scale by appropriately scaling-up all the components. Single crystals suitable for X-ray diffraction were grown from an ethanolic solution of the compound by slow diffusion of toluene.

***N*-(*o*-Carboxyphenyl)-4,6-*O*-ethylidene- $\beta$ -D-glucopyranosylamine (HL<sub>COOH</sub>).** 4,6-*O*-EGP (6.18 g, 30 mmol) and anthranilic acid (4.11 g, 30 mmol) were suspended in ethanol (40 mL) and the reaction mixture was refluxed while stirring for 30 min during which it turned to solid material. This was then cooled to room temperature and the product filtered off, washed with ethanol and dried under vacuum.

† Dedicated to Professor S. J. Lippard on his 60th birthday.

**Table 1** Composition, yield, mp, and elemental analysis data for all the compounds

Compound	Composition	Yield (%)	Mp/°C	Found (Calc.) (%)		
				C	H	N
4,6-O-EGP	C <sub>8</sub> H <sub>14</sub> O <sub>6</sub>	56	174–175	46.33 (46.60)	6.83 (6.84)	—
HL <sub>COOH</sub>	C <sub>15</sub> H <sub>19</sub> NO <sub>7</sub>	71	159–161 <sup>a</sup>	55.26 (55.38)	6.03 (5.89)	3.89 (4.30)
L <sub>F</sub>	C <sub>14</sub> H <sub>18</sub> FNO <sub>5</sub>	42	139–141 <sup>a</sup>	55.64 (56.21)	6.11 (6.06)	4.42 (4.68)
L <sub>Cl</sub>	C <sub>14</sub> H <sub>18</sub> ClNO <sub>5</sub>	33	150–152 <sup>a</sup>	53.37 (53.25)	5.88 (5.74)	4.82 (4.43)
<b>1</b> Na–L <sub>COOH</sub>	C <sub>15</sub> H <sub>18</sub> NNaO <sub>7</sub> ·H <sub>2</sub> O	65	138–140 <sup>a</sup>	49.22 (49.32)	5.85 (5.51)	3.74 (3.83)
<b>2</b> K–L <sub>COOH</sub>	(K <sub>2</sub> C <sub>15</sub> H <sub>18</sub> NO <sub>7</sub> ) <sub>2</sub> ·3H <sub>2</sub> O	70	152–154 <sup>a</sup>	46.20 (46.16)	5.63 (5.42)	3.55 (3.59)
<b>3</b> Mg–L <sub>COOH</sub>	Mg(C <sub>15</sub> H <sub>18</sub> NO <sub>7</sub> ) <sub>2</sub> ·7H <sub>2</sub> O	57	>160 <sup>b</sup>	44.81 (45.11)	6.03 (6.31)	3.31 (3.50)
<b>4</b> Ca–L <sub>COOH</sub>	Ca(C <sub>15</sub> H <sub>18</sub> NO <sub>7</sub> ) <sub>2</sub> ·5H <sub>2</sub> O	84	>170 <sup>b</sup>	46.58 (46.28)	6.08 (5.95)	3.86 (3.60)
<b>5</b> Ba–L <sub>COOH</sub>	Ba(C <sub>15</sub> H <sub>18</sub> NO <sub>7</sub> ) <sub>2</sub> ·4H <sub>2</sub> O	84	>170 <sup>b</sup>	41.97 (42.01)	5.37 (5.17)	3.15 (3.26)
<b>6</b> Cd–L <sub>COOH</sub>	Cd(C <sub>15</sub> H <sub>18</sub> NO <sub>7</sub> ) <sub>2</sub> ·5H <sub>2</sub> O	77	146–149 <sup>a</sup>	42.19 (42.31)	5.86 (5.45)	2.99 (3.29)
<b>7</b> Hg–L <sub>COOH</sub>	Hg(C <sub>15</sub> H <sub>18</sub> NO <sub>7</sub> ) <sub>2</sub> ·2H <sub>2</sub> O	72	146–148 <sup>a</sup>	40.63 (40.71)	4.38 (4.55)	2.90 (3.16)

<sup>a</sup> Compound melted and turned brown. <sup>b</sup> Compound turned brown but did not melt.

**4,6-O-Ethylidene-N-(*o*-fluorophenyl)-β-D-glucopyranosyl-amine (L<sub>F</sub>).** 4,6-O-EGP (0.41 g, 1.99 mmol) and *o*-fluoroaniline (0.20 mL, 2.07 mmol) were suspended in ethanol (7 mL) and a catalytic amount of zinc chloride (0.006 g, 0.04 mmol) was added. The reaction mixture was allowed to reflux for 3 h, then cooled to room temperature. It was concentrated under reduced pressure to about 4 mL and kept overnight at room temperature to yield a solid product which was separated by filtration and the residue then washed with cold ethanol followed by ether and dried *in vacuo*.

**N-(*o*-Chlorophenyl)-4,6-O-ethylidene-β-D-glucopyranosyl-amine (L<sub>Cl</sub>).** This compound was prepared by adopting the procedure given for L<sub>F</sub>, but using 4,6-EGP (0.41 g, 1.99 mmol), *o*-chloroaniline (0.21 mL, 2.00 mmol) and a catalytic amount of zinc chloride (0.006 g). Single crystals of the product suitable for X-ray diffraction study were grown by slow evaporation of the concentrated ethanolic solution.

#### Synthesis of metal ion complexes

**Na–L<sub>COOH</sub> 1.** To a solution of 0.36 g (1.10 mmol) HL<sub>COOH</sub> in 30 mL THF–methanol (5:1 v/v), solid sodium hydroxide 0.045 g (1.125 mmol) was added and allowed to stir at room temperature. After 24 h the stirring was stopped and the reaction mixture concentrated to about 4–5 mL under vacuum followed by addition of ether to precipitate the product. The product was isolated by filtration, re-dissolved in methanol and precipitated using diethyl ether.

**K–L<sub>COOH</sub> 2.** This complex was prepared by adopting the procedure given for Na–L<sub>COOH</sub>, but using 0.30 g (0.92 mmol) of HL<sub>COOH</sub> and 0.68 g (0.91 mmol) of potassium hydroxide. Single crystals suitable for X-ray studies were obtained by slow evaporation of a methanolic solution of the product at 4 °C.

**Mg–L<sub>COOH</sub> 3.** To a clear solution of 0.33 g (1.01 mmol) HL<sub>COOH</sub> in 25 mL THF, 0.11 g (0.51 mmol) of solid Mg(OAc)<sub>2</sub>·4H<sub>2</sub>O was added and the reaction mixture stirred at room temperature for 24 h. A white precipitate of the product was formed during the course of the reaction, which was isolated by filtration and the filtrate concentrated to 4–5 mL followed by addition of an excess of ether to precipitate a second crop.

**Ca–L<sub>COOH</sub> 4.** To a solution of HL<sub>COOH</sub> (0.60 g, 1.85 mmol) in 40 mL of THF, triethylamine (0.26 mL, 1.9 mmol) was added and the reaction mixture stirred at room temperature under N<sub>2</sub> atm for 0.5 h and then CaCl<sub>2</sub>·2H<sub>2</sub>O (0.14 g, 0.92 mmol) was added and stirring continued. In 10 minutes the mixture became light yellow. This was stirred for 18 h at room temperature, concentrated and kept in a deep freezer at –20 °C. After 4 h, 10 mL of ether were added. A white precipitate was formed which was collected after one day and was twice stirred in CHCl<sub>3</sub> to remove NEt<sub>3</sub>·HCl formed during the reaction.

**Ba–L<sub>COOH</sub> 5.** This compound was prepared by a procedure similar to that adopted for 1, but by using 0.33 g (1.01 mmol) of HL<sub>COOH</sub> and 0.16 g (0.49 mmol) Ba(OH)<sub>2</sub>·8H<sub>2</sub>O in 25 mL of THF.

**Cd–L<sub>COOH</sub> 6.** This compound was prepared by a procedure similar to that adopted for 1, but by using 0.33 g (1.01 mmol) of HL<sub>COOH</sub> and 0.13 g (0.47 mmol) Cd(OAc)<sub>2</sub>·2H<sub>2</sub>O in 25 mL THF.

**Hg–L<sub>COOH</sub> 7.** This compound was prepared by a procedure similar to that adopted for 3, but by using 0.32 g (0.98 mmol) HL<sub>COOH</sub> and 0.16 g (0.49 mmol) Hg(OAc)<sub>2</sub> in 25 mL of THF.

Preliminary data including analytical results of all these compounds are listed in Table 1.

#### X-Ray crystallography

Standard procedures were used for mounting the crystals. The diffraction data were collected for 4,6-O-EGP, L<sub>Cl</sub> and K–L<sub>COOH</sub> 2 on a Nonius Kappa CCD machine in the  $\phi$  scan + $\omega$  scan mode using Mo-K $\alpha$  radiation. The structures were solved using SHELXS 97 and refined using SHELXL 97 program packages.<sup>15</sup> The diagrams were generated using ORTEP 3 and PLUTON 98 programs.<sup>16</sup> Full matrix least-squares refinement with anisotropic thermal parameters for all non-hydrogen atoms was used. The hydrogen atoms were treated as riding atoms with fixed thermal parameters. Other details of data collection and structure refinement are provided in Table 2.

CCDC reference number 186/2168.

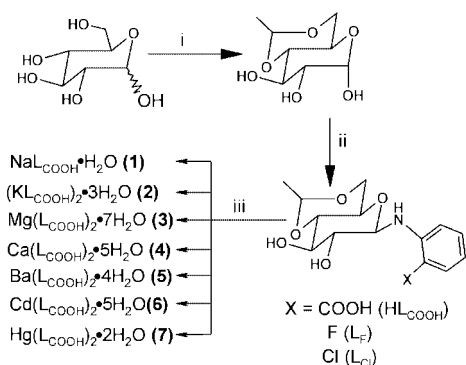
See <http://www.rsc.org/suppdata/dt/b0/b004854m/> for crystallographic files in .cif format.

**Table 2** Summary of crystallographic data for compounds 4,6-O-EGP, L<sub>Cl</sub> and K-L<sub>COOH</sub> 2

	4,6-O-EGP	L <sub>Cl</sub>	K-L <sub>COOH</sub> 2
Empirical formula	C <sub>8</sub> H <sub>14</sub> O <sub>6</sub>	C <sub>14</sub> H <sub>18</sub> ClNO <sub>5</sub>	C <sub>32.5</sub> H <sub>47</sub> K <sub>2</sub> N <sub>2</sub> O <sub>17</sub>
Molecular weight	206.19	315.74	815.92
<i>T</i> / <i>K</i>	173(2)	173(2)	173(2)
Crystal system	Monoclinic	Orthorhombic	Monoclinic
Space group	<i>P</i> 2 <sub>1</sub>	<i>P</i> 2 <sub>1</sub> 2 <sub>1</sub> 2 <sub>1</sub>	<i>C</i> 2
<i>a</i> /Å	5.012(1)	7.056(1)	21.562(1)
<i>b</i> /Å	6.738(1)	12.346(1)	13.501(1)
<i>c</i> /Å	13.748(4)	16.512(1)	15.041(1)
$\beta$ /°	97.31(1)	—	122.07(1)
<i>V</i> /Å <sup>3</sup>	460.51(18)	1438.4(3)	3710.4(4)
<i>Z</i>	2	4	4
Total reflections	1130	7624	10452
Unique reflections	1130 [ <i>R</i> (int) = 0.0000]	4287 [ <i>R</i> (int) = 0.0322]	7437 [ <i>R</i> (int) = 0.0227]
Final <i>R</i> ( <i>I</i> > 2σ( <i>I</i> ))	0.0544	0.0313	0.0375
<i>R</i> <sub>w</sub>	0.1125	0.0754	0.0944

## Results and discussion

Protected glucose, 4,6-O-EGP, its C1–N glycosylated products (HL<sub>COOH</sub>, L<sub>F</sub>, and L<sub>Cl</sub>) and the metal ion complexes of L<sub>COOH</sub> (Na-L<sub>COOH</sub> 1; K-L<sub>COOH</sub> 2; Mg-L<sub>COOH</sub> 3; Ca-L<sub>COOH</sub> 4; Ba-L<sub>COOH</sub> 5; Cd-L<sub>COOH</sub> 6 and Hg-L<sub>COOH</sub> 7) have been synthesized as shown in Scheme 1 and were well characterized.



**Scheme 1** i, Paraldehyde/concentrated H<sub>2</sub>SO<sub>4</sub> (catalyst); ii, suitable *ortho*-substituted aniline and iii, suitable metal salt.

### 4,6-O-Ethylidene-α-D-glucopyranose (4,6-O-EGP)

D-Glucopyranose was protected at its 4 and 6 positions using paraldehyde to result in 4,6-O-EGP as in the Experimental section. <sup>1</sup>H NMR and its D<sub>2</sub>O exchange spectra of this molecule revealed the presence of only three hydroxyl groups observed at δ 6.45, 4.99 and 4.72 respectively. The hydrogen atom attached to C1 was found at δ 4.93 and its *J* value (4.4 Hz) supports the presence of the α anomeric form in the molecule. The <sup>1</sup>H NMR spectrum of this molecule is shown in Fig. 1(a). However, a mixture of anomers was found, based on <sup>1</sup>H NMR, when this α form was left in solution to equilibrate over a period of time. The molecular structure of 4,6-O-EGP based on single crystal X-ray diffraction is shown in Fig. 2(a). The molecule adopts a pyranose structure with positions 4 and 6 being connected by an ethylidene moiety. The stereo view of this molecule shown in Fig. 2(b) also supports the α-anomeric form. The pyranose ring is present in the chair form. Some important bond lengths and bond angles are given in Table 3 and the data does not show any abnormalities. The crystal lattice exhibited five O–H···O type intermolecular hydrogen bonds with O···O distances in the range 2.714–3.160 Å and angles in the range 131.4–174.6°, indicating the presence of intermolecular interactions.

### *ortho*-Substituted aromatic glycosylamines of 4,6-O-ethylidene-α-D-glucopyranose

Three different Cl-glycosylamines are synthesized from the

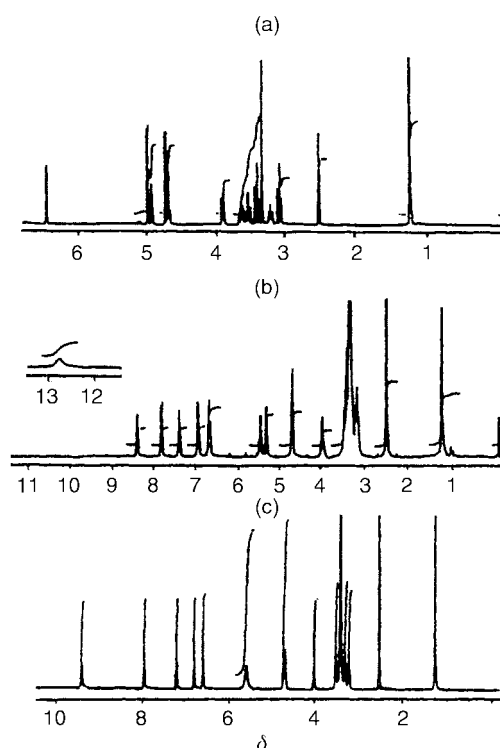


**Fig. 1** <sup>1</sup>H NMR of (a) 4,6-O-EGP, (b) HL<sub>COOH</sub> and (c) Ca-L<sub>COOH</sub> measured in DMSO-d<sub>6</sub>.

reaction of 4,6-O-EGP with anilines substituted in the *ortho*-position by CO<sub>2</sub>H (HL<sub>COOH</sub>), F (L<sub>F</sub>), and Cl (L<sub>Cl</sub>). All these compounds showed satisfactory elemental analysis (Table 1), and were characterized based on FTIR and <sup>1</sup>H NMR spectra. One, L<sub>Cl</sub>, has been structurally characterized by single crystal X-ray diffraction. Formation of glycosylamines was indicated by FTIR spectra where the sharp band originating from the C1–OH stretching vibration (3491 cm<sup>-1</sup>) disappeared as expected. Formation of the glycosylated product was further revealed by comparing its FTIR spectrum with that of the precursor, *i.e.* 4,6-O-EGP. The fingerprint region clearly indicated the presence of an aromatic moiety. In the case of L<sub>COOH</sub>, ν<sub>C=O</sub> was found at 1700 cm<sup>-1</sup>.

In all cases <sup>1</sup>H NMR spectra were recorded in DMSO-d<sub>6</sub> from fresh solutions, since stored solutions exhibited anomeration of the glycosylamine; the corresponding data are given in Table 4. The spectrum of HL<sub>COOH</sub> is shown in Fig. 1(b). The spectra were compared with that of the precursor, *i.e.* 4,6-O-EGP. The <sup>1</sup>H NMR spectra of the glycosylamines showed the presence of only two OH groups from the saccharide moiety and indicated the loss of C1–OH, which was found at δ 6.45

for the precursor molecule 4,6-O-EGP, as expected due to glycosylation at C1. The peak positions of the OH groups were cross-checked by their signal disappearance upon addition of D<sub>2</sub>O. Both the chemical shift ( $\delta$  4.59–4.71) and the  $J$  value for the C1–H (7.5–8.5 Hz) of the glycosylated products clearly supported the presence of the  $\beta$ -anomeric form<sup>13a</sup> in HL<sub>COOH</sub>, L<sub>F</sub>, and L<sub>Cl</sub>. However, the precursor 4,6-O-EGP was found in

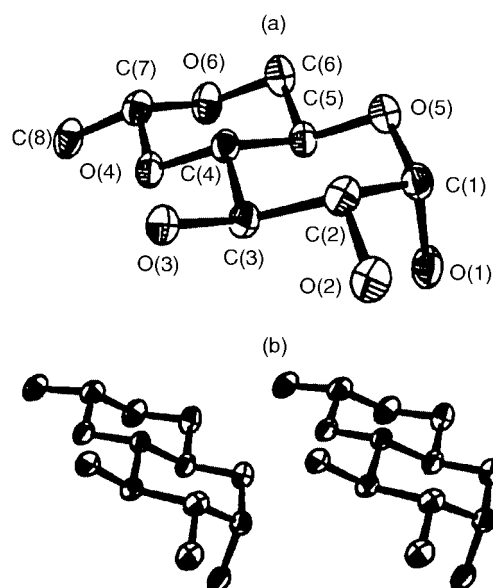


Fig. 2 (a) Molecular structure of 4,6-O-EGP and (b) a stereo view showing 25% probability thermal ellipsoids using ORTEP.

Table 3 Selected bond lengths (Å) and angles (°) for 4,6-O-EGP

O(3)–C(3)	1.433(5)	O(4)–C(7)	1.428(5)
O(4)–C(4)	1.436(4)	O(5)–C(1)	1.423(5)
O(5)–C(5)	1.424(4)	O(6)–C(7)	1.418(5)
O(6)–C(6)	1.425(5)	C(1)–C(2)	1.535(6)
C(2)–C(3)	1.522(5)	C(3)–C(4)	1.498(7)
C(4)–C(5)	1.521(5)	C(5)–C(6)	1.502(7)
C(7)–C(8)	1.501(6)		
C(1)–O(5)–C(5)	111.7(3)	C(7)–O(4)–C(4)	111.0(3)
O(1)–C(1)–O(5)	112.0(3)	C(7)–O(6)–C(6)	111.2(3)
O(5)–C(1)–C(2)	110.1(3)	O(1)–C(1)–C(2)	107.3(3)
O(2)–C(2)–C(1)	111.1(3)	O(2)–C(2)–C(3)	108.4(3)
O(3)–C(3)–C(2)	111.0(3)	O(3)–C(3)–C(4)	109.6(3)
C(4)–C(3)–C(2)	108.8(3)	C(3)–C(2)–C(1)	110.8(3)
O(4)–C(4)–C(5)	108.2(3)	O(4)–C(4)–C(3)	110.5(3)
O(5)–C(5)–C(6)	110.6(3)	C(3)–C(4)–C(5)	110.4(3)
C(6)–C(5)–C(4)	108.0(3)	O(5)–C(5)–C(4)	110.1(3)
O(6)–C(7)–O(4)	111.2(3)	O(6)–C(7)–C(8)	108.3(3)
O(4)–C(7)–C(8)	107.9(4)	O(6)–C(7)–C(8)	108.0(3)

Table 4 <sup>1</sup>H NMR data ( $\delta$ ) for all the compounds recorded in DMSO-*d*<sub>6</sub>

Compound	NH	Saccharide protons		Aromatic protons
		C1–H	OH	
HL <sub>COOH</sub>	8.39	4.71	5.47, 5.32 12.78 (CO <sub>2</sub> H)	6.69 (1H), 6.84 (1H), 7.38 (1H), 7.80 (1H)
L <sub>F</sub>	5.52	4.56	5.27, 5.16	6.63 (1H), 6.95 (3H)
L <sub>Cl</sub>	5.57	4.62	5.35, 5.29	6.71 (1H), 6.93 (1H), 7.15 (1H), 7.28 (1H)
1 Na–L <sub>COOH</sub>	9.83	4.59	5.63	6.51 (1H), 6.71 (1H), 7.09 (1H), 7.81 (1H)
2 K–L <sub>COOH</sub>	9.97	4.56	6.05, 5.64	6.49 (1H), 6.67 (1H), 7.05 (1H), 7.77 (1H)
3 Mg–L <sub>COOH</sub>	9.06	4.65	5.44	6.59 (1H), 6.80 (1H), 7.21 (1H), 7.91 (1H)
4 Ca–L <sub>COOH</sub>	9.38	4.66	5.57	6.57 (1H), 6.77 (1H), 7.17 (1H), 7.93 (1H)
5 Ba–L <sub>COOH</sub>	9.57	4.65	5.70	6.55 (1H), 6.75 (1H), 7.14 (1H), 7.90 (1H)
6 Cd–L <sub>COOH</sub>	9.06	4.64	5.45	6.59 (1H), 6.79 (1H), 7.21 (1H), 7.92 (1H)
7 Hg–L <sub>COOH</sub>	8.78	4.70	5.42, 5.29	6.64 (1H), 6.87 (1H), 7.27 (1H), 7.87 (1H)

C<sub>5</sub>–H of the saccharide molecule was found in the range  $\delta$  3.97–4.00 and the rest of the five skeletal protons in the range  $\delta$  3.00–3.50. CH<sub>3</sub> of the protecting group was found at  $\delta$  1.22–1.25 and its CH at  $\delta$  4.69–4.72.

its  $\alpha$ -anomeric form. Such a change in the anomeric form on going from 4,6-O-EGP to its C1–glycosylamine is in accordance with the low energy conformation expected with the  $\beta$ -anomeric form<sup>13b</sup> in the latter case. The remaining skeletal proton signals appeared in the expected ranges, as given in Table 4.

The molecular structure of L<sub>Cl</sub> based on single crystal X-ray diffraction is shown in Fig. 3(a). It revealed the presence of C1–glycosylation of the saccharide moiety with the corresponding amine. Further, the saccharide moiety maintained its pyranose form with the 4 and 6 positions being protected by the ethylidene moiety as in the structure of the precursor, 4,6-O-EGP. The stereo view of this molecule shown in Fig. 3(b) supports the presence of the  $\beta$ -anomeric form. The glycosylation clearly resulted in a change in the state of the anomeric form from  $\alpha$  to  $\beta$ . Thus the results obtained from the crystal structure are comparable with those obtained from solution studies, based on <sup>1</sup>H NMR spectra. Some important bond lengths and bond angles are given in Table 5. The metric parameters have not shown any abnormalities. The stereo view shown in Fig. 3(b) of this molecule indicates that the *ortho* substituent is oriented in the same direction as that of C2–OH. The pyranose ring is present in the chair form. The orientation of the molecule observed in the lattice was expected to facilitate the binding of metal ions if the *ortho* substituent were to be a group capable of binding (the group that is present in place of Cl). Therefore, among the three glycosylamines reported here, HL<sub>COOH</sub> is suited for metal ion binding, and we report the synthesis, characterisation and crystal structure of metal ion bound products of HL<sub>COOH</sub>. The crystal lattice of L<sub>Cl</sub> exhibited

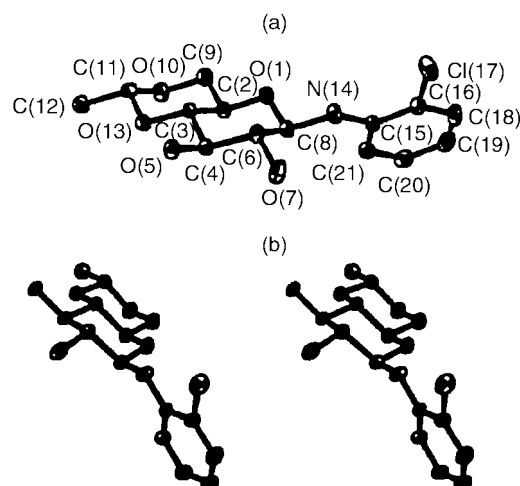


Fig. 3 (a) Molecular structure of L<sub>Cl</sub> and (b) stereo view showing 50% probability level thermal ellipsoids using ORTEP for all non-hydrogen atoms.

**Table 5** Selected bond lengths (Å) and angles (°) for L<sub>Ca</sub>

C(2)–O(1)	1.419(18)	C(2)–C(9)	1.517(2)
C(2)–C(3)	1.531(2)	C(3)–O(13)	1.431(18)
C(3)–C(4)	1.504(2)	C(4)–O(5)	1.428(17)
C(4)–C(6)	1.528(2)	C(6)–O(7)	1.417(19)
C(6)–C(8)	1.533(2)	C(8)–N(14)	1.419(2)
C(8)–O(1)	1.447(18)	C(9)–O(10)	1.436(2)
C(11)–O(10)	1.406(19)	C(11)–O(13)	1.438(17)
C(11)–C(12)	1.497(2)	C(15)–N(14)	1.387(19)
C(16)–Cl(17)	1.742(2)		
O(1)–C(2)–C(9)	110.57(12)	O(1)–C(2)–C(3)	109.37(12)
C(9)–C(2)–C(3)	108.27(12)	O(13)–C(3)–C(4)	110.32(11)
O(13)–C(3)–C(2)	109.17(12)	C(4)–C(3)–C(2)	109.02(12)
O(5)–C(4)–C(3)	108.98(11)	O(5)–C(4)–C(6)	112.42(12)
C(3)–C(4)–C(6)	108.53(12)	O(7)–C(6)–C(4)	110.45(12)
O(7)–C(6)–C(8)	106.93(12)	C(4)–C(6)–C(8)	109.90(13)
N(14)–C(8)–O(1)	108.69(12)	N(14)–C(8)–C(6)	110.82(13)
O(1)–C(8)–C(6)	110.40(11)	O(10)–C(9)–C(2)	107.87(12)
O(10)–C(11)–O(13)	110.08(12)	O(10)–C(11)–C(12)	110.11(14)
O(13)–C(11)–C(12)	107.85(12)	C(15)–N(14)–C(8)	123.53(14)
C(2)–O(1)–C(8)	111.08(11)	C(11)–O(10)–C(9)	111.54(13)
C(3)–O(13)–C(11)	110.85(11)		

two strong O–H···O type intermolecular hydrogen bonds where the two free OH groups of the saccharide moiety act as donors, with O···O distances of 2.785 and 2.956 Å and H-bond angles of 179 and 170.2° respectively, indicating intermolecular interactions.

#### Metal ion complexes of HL<sub>COOH</sub>

A series of metal ion complexes of HL<sub>COOH</sub> has been synthesized using Na<sup>+</sup>, K<sup>+</sup>, Mg<sup>2+</sup>, Ca<sup>2+</sup>, Ba<sup>2+</sup>, Cd<sup>2+</sup> and Hg<sup>2+</sup>. The composition of all these complexes is given in Table 1. All these products were characterized based on FTIR, <sup>1</sup>H NMR spectra and on TGA/DTA analysis. One, K–L<sub>COOH</sub> **2**, has structurally been characterised by single crystal X-ray diffraction.

In the FTIR spectra of the metal ion complexes, **1** to **7**,  $\nu_{C-O}$  was found in the range 1600–1620 cm<sup>-1</sup> whereas in case of the precursor ligand, HL<sub>COOH</sub>,  $\nu_{C-O}$  was found at 1700 cm<sup>-1</sup>. The shift observed supports the participation of the CO<sub>2</sub>H group in complex formation. The spectra observed in the OH stretching vibrational region were broadened when compared to that of the precursor ligand due to the presence of H<sub>2</sub>O in the metal ion complexes.

The metal ion complex formation was further supported by <sup>1</sup>H NMR studies. The corresponding data are given in Table 4. Disappearance of the CO<sub>2</sub>H proton, downfield shift of the NH proton and shifts of the saccharide OH proton signals were some of the general features observed in the <sup>1</sup>H NMR spectra of these complexes. The spectrum of a representative complex Ca–L<sub>COOH</sub> **2** is shown in Fig. 1(c). Both the NH and OH proton signals were identified through D<sub>2</sub>O exchange experiments. In the metal ion complexes, **1** to **7**, the two saccharide OH groups and one NH group were found to retain their protons. The NH proton signals were shifted downfield for the complexes in DMSO-*d*<sub>6</sub> by 0.4 to 1.6 ppm when compared to their position for the precursor ligand, HL<sub>COOH</sub>. Thus the observed shifts in the NH proton signal of the complexes are in the order Hg<sup>2+</sup> < Cd<sup>2+</sup> ≈ Mg<sup>2+</sup> < Ca<sup>2+</sup> < Ba<sup>2+</sup> < Na<sup>+</sup> < K<sup>+</sup>, higher with monovalent ions than with divalent ones. Further, in the case of alkali and alkaline-earth metal ions, in the same group, as the size increases the downfield shift also increases. <sup>1</sup>H NMR spectral data corresponding to the saccharide OH groups clearly indicated that these are not involved in co-ordination in the case of the complexes of cadmium and mercury, **6** and **7**. Combining this result with that of the analytical composition and the chemical nature of the metal ions, it is possible to propose tetrahedral structures for these complexes where the CO<sub>2</sub><sup>-</sup> and NH are bound in **6** and **7**.

Based on <sup>1</sup>H NMR spectra, it was evident that no organic solvent molecules were associated with the metal ion complexes. However the FTIR spectra indicated the presence of H<sub>2</sub>O molecules. The latter was supported by TGA/DTA analysis. The complexes (**1**, **2**, and **4–7**) lost water molecules till about 160 °C, followed by slow decomposition of the organic moiety. Complexes **1**, **2**, **4**, **5**, **6** and **7** lost 1, 3, 5, 4, 5 and 2 molecules of water respectively. In the case of Hg–L<sub>COOH</sub> **7** the weight loss was ≈100% at 685 °C indicating that Hg was vaporised due to the decomposition of HgO. All the other complexes exhibited residual mass (11.3 to 23.5%) indicating the presence of non-volatile products at the end. In the case of the barium complex, **5**, no weight loss were found beyond 500 °C. Thus the presence of H<sub>2</sub>O molecules has been identified based on FTIR, TGA/DTA and elemental analysis. While on the one hand the alkali and alkaline-earth metal ions are hydrophilic, at least some of the water molecules present in these complexes seem to be involved in stabilising the corresponding co-ordination polyhedron as the glycosylamine alone cannot fulfil the co-ordination sphere. However, the co-ordination sphere around each metal ion can be fulfilled by the formation of a polymeric structure incorporating the solvent molecules as demonstrated in case of the potassium complex, **2**, where crystallisation from MeOH resulted in the replacement of some of the water molecules by MeOH.

#### Molecular and lattice structure of K–L<sub>COOH</sub> **2**

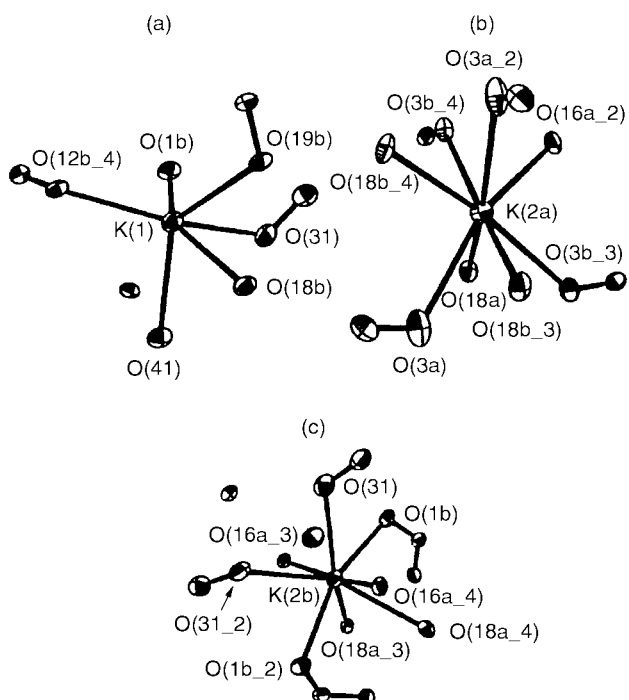
At 4 °C the complex K–L<sub>COOH</sub> **2** crystallised in the monoclinic space group from its methanolic solution resulting in an empirical formula, (KL<sub>COOH</sub>)<sub>2</sub>·2MeOH·H<sub>2</sub>O. This compound exhibited an interesting crystal structure. Two types of potassium ions are present in the asymmetric unit, of which one (K1) has full occupancy whereas the other occupies two positions (K2a and K2b), having occupancy 0.5 each as these two sit on special positions in the unit cell. K1 is co-ordinated to six oxygen atoms giving rise to an octahedral co-ordination sphere. The metric data around K1 clearly indicated distorted octahedral geometry. The co-ordinated oxygen centers for K1 arise from the saccharide as well as from two methanol molecules. One of these methanol molecules bridges between K1 and K2b. K2a and K2b are surrounded by 8 oxygen donor atoms. The co-ordination around each crystallographic potassium ions is shown in Fig. 4(a), (b) and (c). The packing diagram of the unit cell shows an interesting layer type structure, where one layer contains only K1 followed by the next layer, which contains K2a and K2b. A view of the lattice structure of this complex is shown in Fig. 5. K2b and K1 are connected *via* bridging carboxylic oxygen as well as methanol oxygens. The binding mode of the ligand L<sub>COOH</sub> towards K<sup>+</sup> ions in the lattice is shown in Fig. 6. Thus both the glycosylamine moiety and MeOH are responsible for the formation of the layered type polymeric structure. Selected bond lengths and bond angles about each potassium ion center are given in Table 6. The potassium–oxygen distances in all the three co-ordination spheres are in the range 2.721 to 3.046 Å, with an average of 2.861 Å. These bond lengths are well consistent with literature values for KO<sub>6</sub> and KO<sub>8</sub> systems.<sup>17</sup>

#### Conclusion

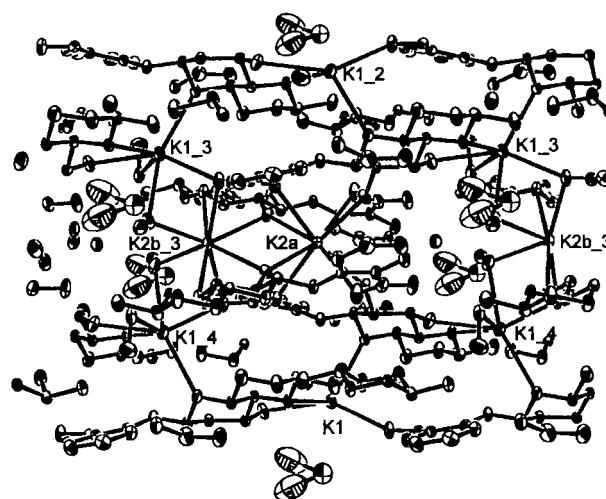
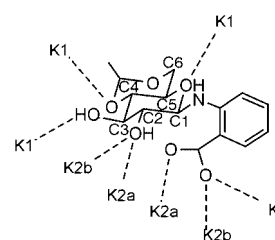
A successful systematic approach has been reported in this paper to synthesize saccharide based ligands suitable for metal ion binding. Glucose has partially been protected to result in 4,6-O-EGP in the  $\alpha$ -anomeric form. The presence of the  $\alpha$ -anomeric form of glucose in 4,6-O-EGP has been established based on <sup>1</sup>H NMR as well as single crystal XRD study. A few analogous glycosylamines based on 4,6-O-EGP have also been synthesized and were well characterised. Although 4,6-O-EGP was in the  $\alpha$ -anomeric form, <sup>1</sup>H NMR of the glycosylamines indicated the presence of the  $\beta$ -anomeric form. The presence of

**Table 6** Selected bond lengths (Å) and angles (°) for K-L<sub>COOH</sub>

K(1)–O(1B)	2.721(2)	K(1)–O(31)	2.750(2)
K(1)–O(16B)	2.821(2)	K(1)–O(41)	2.926(2)
K(1)–O(12B_4)	2.936(18)	K(1)–O(19B)	3.046(19)
K2a–O3a, K2a–O3a_2	2.983(2)	K2a–O3b_3, K2a–O3b_4	2.930(19)
K2a–O18a, K2a–O18a_2	2.722(18)	K2a–O18b_3, K2a–O18b_4	2.754(18)
K2b–O1b, K2b–O1b_2	2.870(2)	K2b–O16a_3, K2b–O16a_4	2.815(19)
K2b–O18a_3, K2b–O18a_4	2.985(19)	K2b–O31, K2b–O31_2	2.815(2)
O1b–K1–O31	70.85(7)	O1b–K1–O16b	145.56(6)
O1b–K1–O41	115.52(6)	O1b–K1–O12b_4	88.66(6)
O1b–K1–O19b	108.97(6)	O31–K1–O41	85.49(6)
O31–K1–O16b	75.12(6)	O31–K1–O12b_4	159.16(6)
O31–K1–O19b	78.73(6)	O16b–K1–O41	66.00(6)
O16b–K1–O12b_4	125.61(6)	O16b–K1–O19b	58.20(5)
O41–K1–O12b_4	100.59(6)	O41–K1–O19b	124.15(5)
O12b_4–K1–O19b	112.73(5)	O18a–K2a–O18a_2	85.93(8)
O18a–K2a–O18b_3, O18a_2–K2a–O18b_4	115.32(6)	O18a–K2a–O18b_4, O18a_2–K2a–O18b_3	125.28(6)
O18a–K2a–O3b_3, O18a_2–K2a–O3b_4	55.18(5)	O18a–K2a–O3b_4, O18a_2–K2a–O3b_3	74.72(5)
O18b_3–K2a–O18b_4	93.23(8)	O18b_3–K2a–O3b_3, O18b_4–K2a–O3b_4	78.43(5)
O18b_4–K2a–O3b_3, O18b_3–K2a–O3b_4	169.73(6)	O18b_4–K2a–O3a, O18b_3–K2a–O3a_2	83.74(6)
O18_4–K2a–O3a_2, O18b_3–K2a–O3a	52.89(5)	O3b_3–K2a–O3b_4	110.47(7)
O3a_2–K2a–O3b_3	130.84(5)	O3a_2–K2a–O3b_4, O3a–K2a–O3b_3	86.42(5)
O18a–K2a–O3a_2	160.58(6)	O18a–K2a–O3a, O18a_2–K2a–O3a_2	79.39(6)
O3a–K2a–O3a_2	117.52(9)	O16a_3–K2b–O16a_4	168.69(9)
O16a_3–K2b–O31, O16a_4–K2b–O31_2	91.29(6)	O16a_4–K2b–O31, O16a_3–K2b–O31_2	79.59(6)
O31–K2b–O31_2	73.30(9)	O16a_3–K2b–O1b_2, O16a_4–K2b–O1b	108.02(5)
O16a_3–K2b–O1b, O16a_4–K2b–O1b_2	74.10(5)	O31–K2b–O1b_2, O31_2–K2b–O1b	131.81(6)
O31–K2b–O1b, O31_2–K2b–O1b_2	67.79(6)	O1b–K2b–O1b_2	159.27(8)
O16a_4–K2b–O18a_4, O16a_3–K2b–O18a_3	58.03(5)	O16a_4–K2b–O18a_3, O16a_3–K2b–O18a_4	133.15(6)
O31–K2b–O18a_3, O31_2–K2b–O18a_4	139.59(5)	O31–K2b–O18a_4, O31_2–K2b–O18a_3	119.71(5)
O1b–K2b–O18a_4, O1b_2–K2b–O18a_3	85.70(5)	O1b–K2b–O18a_3, O1b_2–K2b–O18a_4	78.06(5)
O18a_3–K2b–O18a_4	76.84(7)		

**Fig. 4** Co-ordination around (a) K1, (b) K2a and (c) K2b in the molecular structure of K-L<sub>COOH</sub> generated from ORTEP showing 50% probability level thermal ellipsoids.

the latter form in one of the glycosylamines (L<sub>C1</sub>) has been confirmed from single crystal X-ray study. The structure of the C(1)-glycosylamine has indicated a suitable orientation for metal binding utilising the OH groups of the saccharide and the *ortho* substituent. Complexes of Na<sup>+</sup>, K<sup>+</sup>, Mg<sup>2+</sup>, Ca<sup>2+</sup>, Ba<sup>2+</sup>, Cd<sup>2+</sup> and Hg<sup>2+</sup> have been synthesized with one of the glycosylamines (HL<sub>COOH</sub>) and were characterized using various analytical and spectral means, and in the case of K-L<sub>COOH</sub> **2** also by single crystal X-ray study. Thus during the present study molecular and crystal structures of the starting precursor

**Fig. 5** 3-D Molecular structure of K-L<sub>COOH</sub> showing the layer type structure obtained from ORTEP 50% probability level thermal ellipsoids for all non-hydrogen atoms.**Fig. 6** Binding mode of L<sub>COOH</sub> towards K<sup>+</sup> ions; C1, C2, C3, C4, C5 and C6 denote the numbering system followed for the glucose moiety.

(4,6-O-EGP), a glycosylamine (L<sub>C1</sub>), and a metal ion complex (K-L<sub>COOH</sub>) were established. In the structure of K-L<sub>COOH</sub> it was found that primarily oxygen atoms participate in the co-ordination. While the carboxyl group is bound to the metal ion

as carboxylate, the OH groups of the saccharide interacted without deprotonation in the case of the alkali and alkaline-earth metal ion complexes, 1–5. However, in 6 and 7 the saccharide OH group is not bound to the metal ion. These molecules are potentially suitable for complexation with transition metal ions as well and corresponding studies are currently underway in our laboratory.

### Acknowledgements

C. P. R. acknowledges financial support from the Department of Science and Technology, Board of Research in Nuclear Sciences of Department of Atomic Energy and Council of Scientific and Industrial Research. We thank Dr A. Ramanan, IIT Delhi for TGA/DTA data.

### References

- 1 J. F. Kennedy and C. A. White, *Bioactive Carbohydrates in Chemistry, Biochemistry and Biology*, John Wiley and Sons, New York, 1983.
- 2 S. J. Lippard and J. M. Berg (Editors), *Principles of Bioinorganic Chemistry*, University Science Books, Mill Valley, CA, 1994.
- 3 R. P. Bandwar and C. P. Rao, *Curr. Sci.*, 1997, **72**, 788 and refs. therein.
- 4 S. Yano and K. Ohtsuka, in *Metal ions in biological systems*, eds. H. Sigel and A. Sigel, Marcel Dekker, New York, 1996, vol. 32, p. 27 and refs. therein.
- 5 D. M. Whitfield, S. Stojkovsk and B. Sarkar, *Coord. Chem. Rev.*, 1993, **122**, 171 and refs. therein.
- 6 U. Piarulli and C. Floriani, *Prog. Inorg. Chem.*, 1997, **45**, 393 and refs. therein.
- 7 S. Yano, *Coord. Chem. Rev.*, 1998, **92**, 113 and refs. therein.
- 8 D. Steinborn, H. Junicke and C. Bruhn, *Angew. Chem., Int. Ed. Engl.*, 1997, **36**, 2686; H. Junicke, C. Bruhn, D. Strohl, R. Kluge and D. Steinborn, *Inorg. Chem.*, 1998, **37**, 4603; H. Junicke, C. Bruhn, R. Kluge, A. S. Serianni and D. Steinborn, *J. Am. Chem. Soc.*, 1999, **121**, 6232.
- 9 U. Piarulli, D. N. Williams, C. Floriani, G. Gervasio and D. Viterbo, *J. Chem. Soc., Chem. Commun.*, 1994, 1409; U. Piarulli, D. N. Williams, C. Floriani, G. Gervasio and D. Viterbo, *J. Chem. Soc., Dalton Trans.*, 1995, 3329; U. Piarulli, C. Floriani, N. Re, G. Gervasio and D. Viterbo, *Inorg. Chem.*, 1998, **37**, 5142.
- 10 R. O. Duthaler, P. Herold, W. Lottenbach, K. Oertle and M. Riediker, *Angew. Chem., Int. Ed. Engl.*, 1989, **28**, 495; G. Bold, R. O. Duthaler and M. Riediker, *Angew. Chem., Int. Ed. Engl.*, 1989, **28**, 497; M. Riediker, A. Hafner, U. Piantini, G. Rihs and A. Togni, *Angew. Chem., Int. Ed. Engl.*, 1989, **28**, 499.
- 11 R. Wegner, M. Gottschaldt, H. Görls, E.-G. Jäger and D. Klemm, *Angew. Chem., Int. Ed. Engl.*, 2000, **39**, 595.
- 12 S. Yano, S. Inoue, Y. Yasuda, T. Tanase, Y. Mikata, T. Kakuchi, T. Tsubomura, M. Yamasaki, I. Kinoshita and M. Doe, *J. Chem. Soc., Dalton Trans.*, 1999, 1851; T. Tanase, T. Onaka, M. Nakagoshi, I. Kinoshita, K. Shibata, M. Doe, J. Fujii and S. Yano, *Inorg. Chem.*, 1999, **38**, 3150; T. Tanase, Y. Yasuda, T. Onaka and S. Yano, *J. Chem. Soc., Dalton Trans.*, 1998, 345 and refs. therein; S. Yano, Y. Sakai, K. Toriumi, T. Ito, H. Ito and S. Yoshikawa, *Inorg. Chem.*, 1985, **24**, 498.
- 13 (a) S. P. Gaucher, S. F. Pedersen and J. A. Leary, *J. Org. Chem.*, 1999, **64**, 4012; (b) I. L. Finar, *Organic Chemistry Volume 2: Stereochemistry and the chemistry of natural products*, Fifth Edition, Longman Scientific & Technical, Essex, 1975.
- 14 R. Barker and D. L. MacDonald, *J. Am. Chem. Soc.*, 1960, **82**, 2301.
- 15 SHELXL 97 Programs for Crystal Structure Analysis (Release 97-2), G. M. Sheldrick, Institut für Anorganische Chemie der Universität Göttingen, 1998.
- 16 M. N. Burnett and C. K. Johnson, ORTEP III, Report ORNL-6895, Oak Ridge National Laboratory, Oak Ridge, TN, 1996; A. L. Spek, *Acta Crystallogr., Sect. A*, 1990, **46**, C34.
- 17 C. Cambillau, G. Bram, J. Corset, C. Riche and C. Pascard-Billy, *Tetrahedron*, 1978, **34**, 2675; C. L. Liotta, M. L. McLaughlin, D. G. Vanderveer and B. A. O'Brien, *Tetrahedron Lett.*, 1982, **295**, 526; J. A. Bandi, A. Berry, M. L. H. Green, R. N. Perutz, K. Prout and J. N. Verpeaux, *J. Chem. Soc., Chem. Commun.*, 1984, 729; R. B. Dyer, R. G. Ghirardelli, R. A. Palmer and E. M. Holt, *Inorg. Chem.*, 1986, **25**, 3184; M. E. Fraser, S. Fortier, M. K. Markiewicz, A. Rodrigue and J. W. Bovenkamp, *Can. J. Chem.*, 1987, **65**, 2558; D. Lamba, W. Mackie, B. Sheldrick, P. Belton and S. Tanner, *Carbohydr. Res.*, 1988, **180**, 183.